Inventory of Supplementary Materials

Figure S1, related to Figure 1. Characterization of an *irx7*:GFP gene-trap line shows continued expression of *irx7* at the hyoid joint. Analysis of a Bmp4 misexpression line shows a specific role of Bmp signaling in hyoid joint formation and *irx7* regulation.

Figure S2, related to Figure 2. Validation of *irx7* and *irx5a* phenotypes with independent alleles. Quantitation of chondrocyte number shows a role of Irx7 and Irx5a in the morphogenesis of the symplectic cartilage. Lack of cross-regulation in *irx7* and *irx5a* mutants.

Figure S3, related to Figure 3. Potential evolutionary history of *irx7* shows how it might have been lost from tetrapod genomes.

Figure S4, related to Figure 4. Characterization of mutant versions of the R2 enhancer shows that deletion of the first Irx site results in ectopic expression at multiple joints. Analysis of pectoral fin joint and mouse digit joint shows expression of Irx1 genes at these joints.

Movie S1 Legend. Real-time movie of a lightly anesthetized *sox10*:dsRed transgenic zebrafish larva at 21 dpf shows hinge-like movements of ceratohyal and hyosymplectic cartilages around the hyoid joint (arrow) during respiration.

Supplementary Experimental Procedures. This section describes the creation of transgenic and mutant lines used in this study, as well as expanded details on ATDC5 cell experiments.

Supplementary References. Related to Supplementary Experimental Procedures.

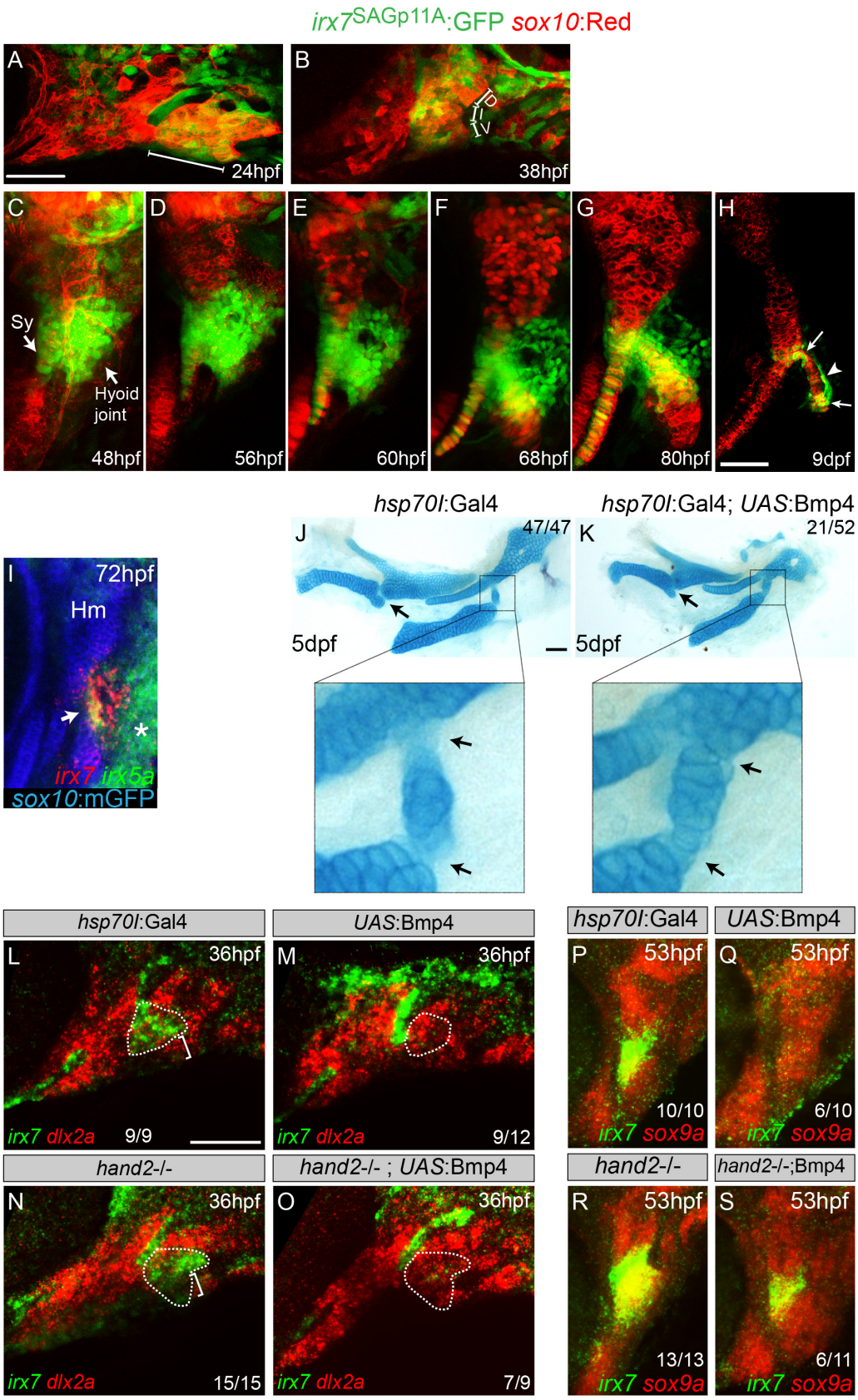
irx7SAGp11A:GFP sox10:Red
A
24hpf
B
D
V
38hpf
C
Sy
Hyoid joint
48hpf
D
56hpf
E
60hpf
F
68hpf
G
80hpf
H
9dpf
hsp70l:Gal4
hsp70l:Gal4; UAS:Bmp4
I
72hpf
Hm
irx7 irx5a
sox10:mGFP
J
47/47
5dpf
K
21/52
5dpf
hsp70l:Gal4
UAS:Bmp4
L
36hpf
irx7 dlx2a
9/9
M
36hpf
irx7 dlx2a
9/12
hsp70l:Gal4
UAS:Bmp4
P
53hpf
10/10
irx7 sox9a
Q
53hpf
6/10
irx7 sox9a
hand2-/-
hand2-/- ; UAS:Bmp4
N
36hpf
irx7 dlx2a
15/15
O
36hpf
irx7 dlx2a
7/9
hand2-/-
hand2-/-;Bmp4
R
53hpf
13/13
irx7 sox9a
S
53hpf
6/11
irx7 sox9a

Figure S1, Related to Figure 1. Progressive restriction of *irx7*:GFP to the hyoid joint and Hand2-independent inhibition of *irx7* expression by Bmp signaling.

(A-H) Confocal projections of the mandibular and hyoid arches at 24 (A), 38 (B), and 48 hpf (C) and the hyoid cartilages at 56 hpf onwards (D-H). *sox10*:mCherryCAAX (24, 48, 56, and 80 hpf and 9 dpf) and *sox10*:dsRed (38, 60, and 68 hpf), collectively abbreviated as "*sox10*:Red", mark neural-crest-derived arch mesenchyme and later chondrocytes in red. The SAGp11A line is an insertion of a GFP-containing retrotransposon into the second exon of the *irx7* gene. *irx7*-driven GFP expression is seen weakly throughout the hyoid arch at 24 hpf (A) and then becomes refined to the intermediate domain of the hyoid arch by 38 hpf (B). Expression then increases in the hyoid joint and adjacent symplectic cartilage region by 48 hpf (C). At later times, GFP expression persists around the hyoid joint but is gradually lost in the growing symplectic cartilage (D-G). In mid-stage larvae (9 dpf), GFP is highly restricted to chondrocytes at either end of the bipartite hyoid joint (arrows), as well as in perichondral cells (arrowhead) lining the joint (H).

(I) At 72 hpf, relative to *sox10*:GFPCAAX+ cartilages (anti-GFP, blue), overlapping expression of *irx7* (red) and *irx5a* (green) is seen at the developing hyoid joint (arrow). *irx5a* is also expressed in posterior hyoid arch cells (asterisk).

(J,K) Alcian blue labeling of cartilage in control *hsp70I*:Gal4 and *hsp70I*:Gal4; *UAS*:Bmp4 animals subjected to a heat shock from 40-44 hpf. Misexpression of Bmp4 at this stage causes joint fusions (arrows, see magnification of hyoid joint) in the absence of

the large-scale dorsoventral patterning defects caused by earlier (20-24 hpf) induction of Bmp4 (Zuniga et al., 2011).

(L-O) Control *hsp70I*:Gal4 (L), *hsp70I*:Gal4; *UAS*:Bmp4 (M), *hand2*$^{-/-}$ (N), and *hand2*$^{-/-}$; *hsp70I*:Gal4; *UAS*:Bmp4 (O) embryos subjected to a heat shock from 20-24 hpf. In situ hybridization shows ventral expansion (brackets) of *irx7* expression in *hand2*$^{-/-}$ embryos, and loss of hyoid joint expression (dashed polygons) upon Bmp4 misexpression in both wild-type and *hand2* mutant backgrounds. As a reference, *dlx2a* expression labels mandibular and hyoid arch mesenchyme in red.

(P-S) Control *hsp70I*:Gal4 (P), *hsp70I*:Gal4; *UAS*:Bmp4 (Q), *hand2*$^{-/-}$ (R), and *hand2*$^{-/-}$; *hsp70I*:Gal4; *UAS*:Bmp4 (S) embryos subjected to a heat shock from 40-44 hpf. In situ hybridization shows ventral expansion of *irx7* expression in *hand2*$^{-/-}$ embryos, and loss of hyoid joint expression upon Bmp4 misexpression. Loss of *hand2* partially restores some *irx7* expression upon Bmp4 misexpression, suggesting that Bmp4 may act through both Hand2 and other effectors at this later stage. As a reference, *sox9a* expression labels newly forming chondrocytes in red. D, dorsal; I, intermediate; V, ventral; Hm, hyomandibula. Numbers indicate proportion of animals showing the displayed phenotype. Scale bars = 50 μM.

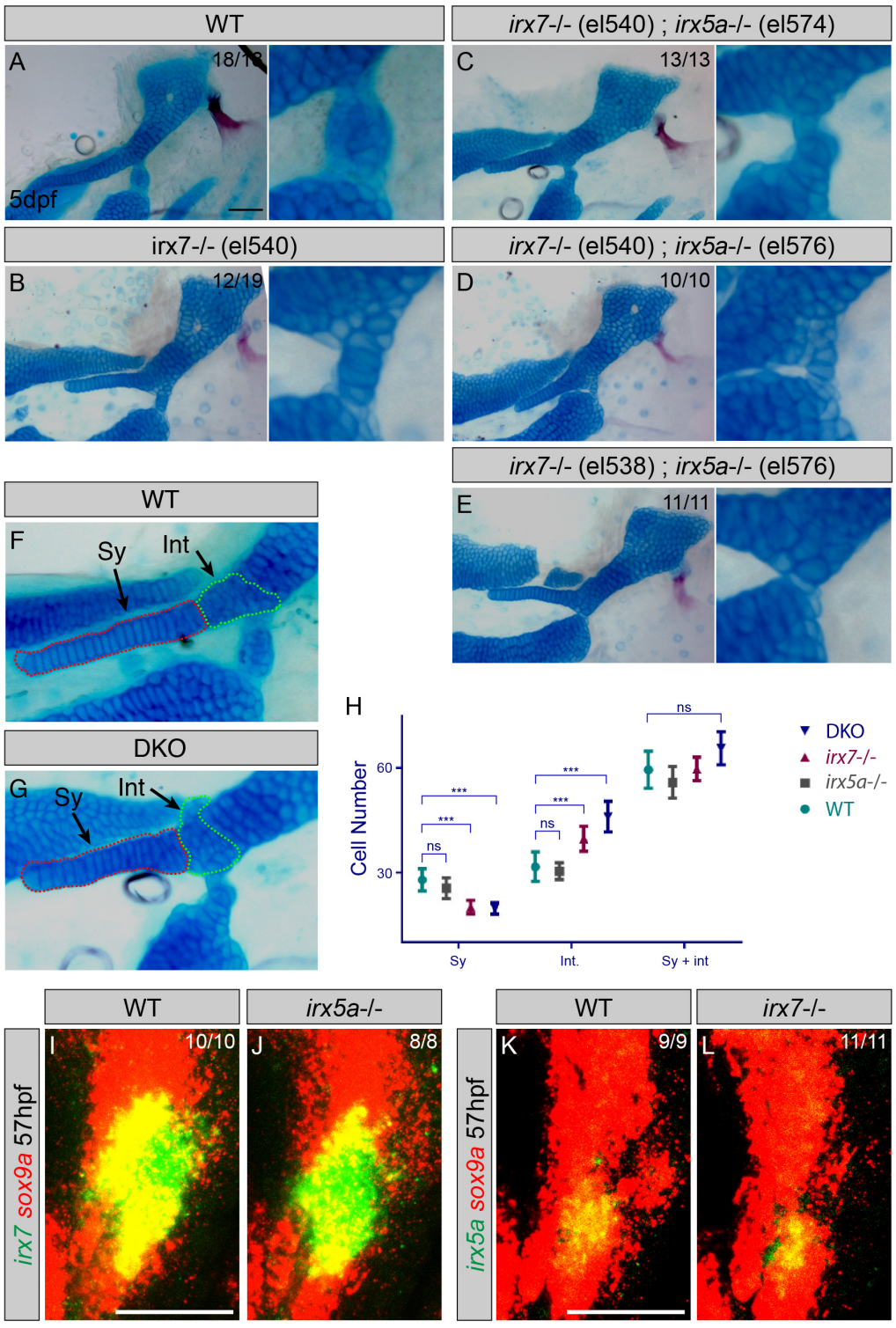

Figure S2, Related to Figure 2. Hyoid joint and symplectic cartilage defects in independent null alleles for *irx7* and *irx5a*.

(A-E) Lateral views of hyoid skeletons (left) and magnified views of hyoid joints (right) show cartilages (Alcian Blue) and bones (Alizarin Red) at 5 dpf. Similar to the *irx7*^{el538} allele (Figure 2D), an independent *irx7*^{el540} allele shows fusions of the hyoid joint (B). All allelic combinations of *irx7*^{el538} or *irx7*^{el540} with *irx5a*^{el574} or an independent *irx5a*^{el576} allele show fully penetrant hyoid joint defects (compare C-E to Figure 2E).

(F,G) Lateral views of dissected hyoid joints and symplectic cartilage (Sy, red dashed line) in *irx7*^{el538}; *irx5a*^{el574} double knock-outs (DKO) and wild-type siblings. The intermediate region between the symplectic and hyomandibular cartilages (Int, green dashed line) was outlined based on the cell shape and stacking difference from the symplectic and hyomandibula proper.

(H) Average cell counts in the Sy, Int, and combined Sy + Int regions are plotted. There were fewer cells in Sy and more cells in Int in *irx7*^{el538} and *irx7*^{el538}; *irx5a*^{el574} DKO embryos compared to wild types, yet no differences in the combined numbers of cells. Cell counts were indistinguishable between wild types and *irx5a*^{el574} animals for all categories. *n* numbers: 8 wild type, 8 *irx5a*$^{-/-}$, 16 *irx7*$^{-/-}$, and 15 DKO; means are shown with 95% CI bars; *** = significant with $\alpha<0.05$ using Tukey-Kramer HSD test; ns = not statistically significant.

(I-L) In situ hybridization at 57 hpf shows expression of *irx7* and *irx5a* (green) relative to *sox9a*+ cartilages (red). *irx7* expression is unaffected in *irx5a*^{el574} mutants, and *irx5a*

expression is unaffected in *irx7*^{el538} mutants. Thus, at least at the level of *irx7* and *irx5a*, there is no genetic compensation in the respective mutants. Numbers indicate proportion of animals showing the displayed phenotype. Scale bar = 50 μM.

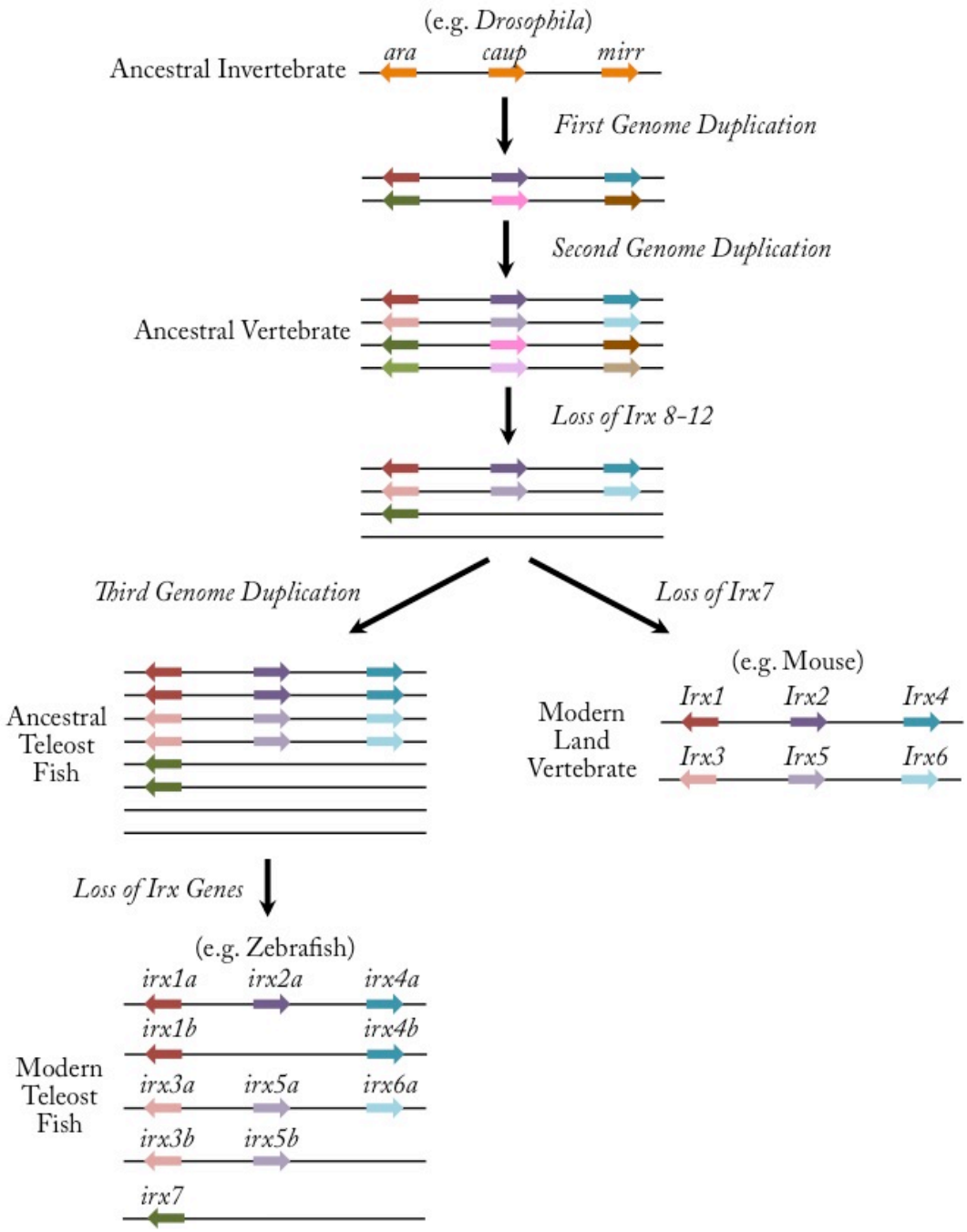

Figure S3, Related to Figure 3. Potential evolutionary history of vertebrate Iroquois genes. Two genome duplication events during vertebrate evolution resulted in four

clusters of Irx genes from the one ancestral invertebrate gene cluster (presumably reflected in the genome of the modern invertebrate *Drosophila melanogaster*). Two of these clusters were maintained intact in ancestral vertebrates together with one gene of a third cluster (*Irx7*). In the teleost fish lineage, a third genome duplication occurred followed by selective loss of some paralogs. In the transition to land, *Irx7* was lost.

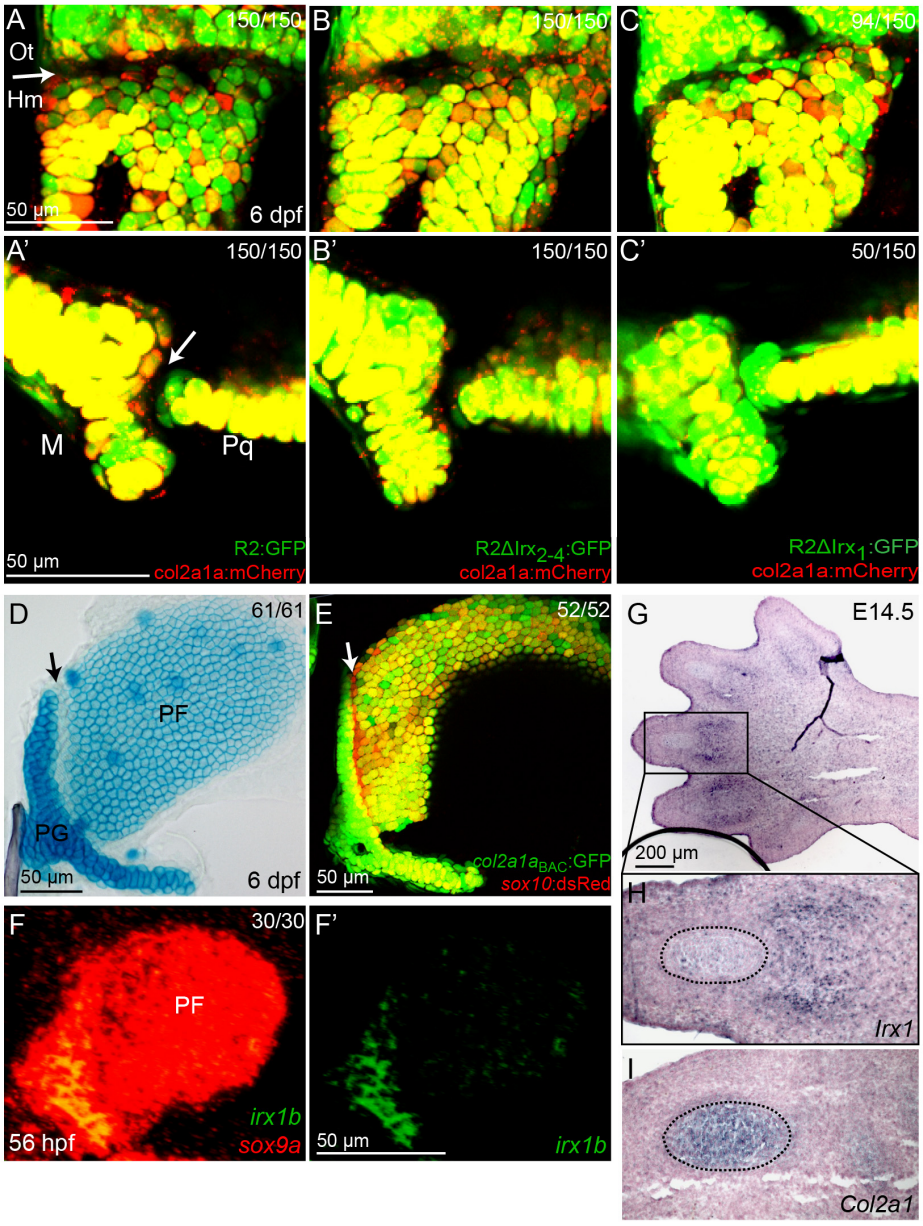

Figure S4, Related to Figure 4. Potential roles of Irx genes at multiple joints.

(A-C) Modified R2 enhancer transgenes (green) are shown relative to a wild-type c*ol2a1a*$_{BAC}$:mCherry-NTR transgene (red) which labels chondrocytes but is excluded from joints (arrows). Compared to the control wild type R2 (A,A'), expression from an R2 enhancer lacking the first Irx site is expanded into the hyomandibula – (Hm) otic capsule (Ot) joint (C) and jaw joint (C'). In contrast, loss of the second through fourth Irx sites has no effect on R2 enhancer expression at these joints (B,B'). Experimental numbers are pooled for three independent stable transgenic lines. 50 embryos were examined for each line. M, Meckel's lower jaw cartilage; Pq, palatoquadrate upper jaw cartilage.

(D-F) The joint between the pectoral fin (PF) and pectoral girdle (PG) shares some of the features of the hyoid joint. At 6 dpf, cells within the pectoral fin joint stain poorly with Alcian Blue relative to surrounding chondrocytes (D, arrow). The pectoral fin joint (arrow) also expresses much lower levels of *col2a1a*$_{BAC}$:GFP relative to surrounding chondrocytes, while *sox10*:dsRed (red) uniformly labels chondrocytes (E). At 56 hpf, *irx1b* is expressed within precursors of the pectoral fin joint (F). *sox9a* expression (red) labels early chondrocytes at this stage. Numbers indicate proportion of animals showing the displayed phenotype.

(G-I) in situ hybridization shows expression of *Irx1* in the digit joints in an E14.5 mouse hindpaw. Magnifications of adjacent sections (H,I) show that *Irx1* and *Col2a1* are expressed in a largely mutually exclusive pattern, with *Col2a1* but not *Irx1* marking cartilage condensations (dashed lines). Serial sections of 2 animals gave similar results.

Movie S1, Related to Figure 1. Real-time movie of a lightly anesthetized *sox10*:dsRed transgenic zebrafish larva at 21 dpf shows hinge-like movements of ceratohyal and hyosymplectic cartilages around the hyoid joint (arrow) during respiration.

Supplementary Experimental Procedures

Tol2 transgenic lines

*sox10:*GFPCAAX and *sox10:*mCherryCAAX plasmids were made by an LR recombination reaction (Gateway; Life Technologies) according to manufacturer instructions. A previously described p5E-*sox10* plasmid (Das and Crump, 2012) was used as promoter. pME-EGFPCAAX (#384) or pME-mCherryCAAX (#550), p3E-polyA (#302), and pDestTol2pA2 (#394) from Tol2kit (Kwan et al., 2007) were used as middle entry, 3' entry, and destination vectors, respectively. *att*B1-Irx7-T2A-GFP-*att*B2 sequence was generated by overlap-extension PCR. The following primers were used in overlap-extension PCR:

*att*B1_irx7_fwd1	GGGGACAAGTTTGTACAAAAAAGCAGGCTCCCGGCCACCATGCCTGCTTCATCAACGGGGTTTGC
T2A_irx7_OE_rev1	CCACGTCACCGCATGTTAGAAGACTTCCTCTGCCCTCTCCTGATCCTTGACTTTGTTTGAGAAGGTCG
T2A_GFP_OE_fwd1	GAGGAAGTCTTCTAACATGCGGTGACGTGGAGGAGAATCCCGGCCCTATGGTGAGCAAGGGCGAGGAGC
*att*B2_GFP_STOP_rev1	GGGGACCACTTTGTACAAGAAAGCTGGGTCTCACTTGTACAGCTCGTCCATGCC

The PCR product was gel purified and cloned into pDONR221 using BP Gateway cloning (Life Technologies) to make the middle entry vector (pME-Irx7-T2A-GFP). In a Gateway LR reaction, pME-Irx7-T2A-GFP was combined with Tol2kit plasmids p5E-UAS (#327), p3E-polyA (#302), and pDestTol2AB2 (Zuniga et al., 2011) to make the *UAS:*Irx7-T2A-GFP; *α-crystallin:*Cerulean plasmid. In each case, the plasmids were sequence verified and injected into one-cell-stage embryos together with Tol2 mRNA to generate stable lines. *Tg(sox10:GFPCAAX)*, and *Tg(sox10:mCherryCAAX)* lines were screened carefully based on previously described expression patterns (Das and Crump, 2012) to ensure neural crest and cartilage expression of the transgene. Three independent stable alleles for *Tg(UAS:Irx7-T2A-GFP; α-crystallin:Cerulean)* were crossed to *hsp70I:*Gal4 and found to similarly inhibit cartilage development upon heat shock at 30-34 hpf. *Tg(UAS:Irx7-T2A-GFP; α-crystallin:Cerulean^{el613})* was used for the transplant experiments.

BAC transgenic lines

The *col2a1a$_{BAC}$:GFP* and *col2a1a$_{BAC}$:mCherry-NTR* transgenic lines were generated by tagging BAC DKEY-152H5 according to published protocols (Shin et al., 2003), with minor modifications. The 5' and 3' homology arms were generated by PCR amplification using the following primer pairs: *att*B4F-PacI-Col2a1-B with *att*B1R-Col2a1-C (5' homology arm) and *att*B2-Col2a1-D with *att*B3R-AscI-Col2a1-E (3' homology arm). *att* sites were added to the primers to facilitate gateway cloning (Life Technologies) and PacI and AscI restriction endonuclease sites were added external to the completed targeting construct. The PCR amplified 5' and 3' homology arm fragments were cloned

into pDONR_P4-P1R and pDONR_P2R-P3 vectors by BP recombination to give 5' and 3' homology arm entry clones. A 1681 bp fragment including SnaBI-polyA-FRT-KanR-FRT-SpeI was excised from the pPCR-eGFPkan plasmid (Shin et al., 2003) and cloned into pME:MCS (Tol2kit, #237) to give pBAC:ME. eGFP or mCherry-NTR were cloned by PCR amplification within KpnI-EcoRI sites upstream of the polyA-FRT-KanR-FRT cassette into the pBAC:ME vector. The mCherry-NTR construct, used as PCR template, was a gift from Ken Poss (Singh et al., 2012). The 5', 3' and middle entry clones were then recombined into the pDestTol2pA2 destination vector (Tol2kit, #394) with an LR reaction. Finally, the PacI-AscI fragment containing the 5' and 3' homology arms on either side of the fluorescent protein was used for homologous recombination with the BAC. Following primer sequences were used in this procedure:

*att*B4F-PacI-Col2a1-B	GGGGACAACTTTGTATAGAAAAGTTGttaattaa GGAATCTTCATAAGTGTATCATGATGTATCA TGTG
*att*B1R-Col2a1-C	GGGGACTGCTTTTTTGTACAAACTTGGTCT AAAGATTAGACATGCAGGTCCTAAGG
*att*B2-Col2a1-D	GGGGACAGCTTTCTTGTACAAAGTGGCTGC TACTTGTGGCAACGCATAGC
*att*B3R-AscI-Col2a1-E	GGGGACAACTTTGTATAATAAAGTTGggcgcgc cCGGGAAGAGCAGAGTTGCTATAGC
KpnI-GFP:FP	gatcaggtaccCGGCCACCATGGTGAGCAAGGGC GAGGAG
EcoRI-GFP:RP	gatcagaattcTTACTTGTACAGCTCGTCCATGCC G
KpnI-mCherry:FP	GATCGGGTACCATGGTGAGCAAGGGCGAG GAGGA
SalI-NTR:RP	GATCGGTCGACTCACACCTCGGTCAGGGTG ATGTTC

TALEN mutants

Two pairs of Transcription Activator-Like Effector Nucleases (TALENs) were designed and constructed based on a previously described protocol (Sanjana et al., 2012). Target sequences for each TALEN were as follows: TGGACAGAAACATCAACATG for the *irx7* 5' TALEN, ATTAGGCTGCCCACCTGGAA for the *irx7* 3' TALEN, TGCTCCCCTGGGCTCGTACC for the *irx5a* 5' TALEN, and CGCAAGAATGCTACCCGGGA for the *irx5a* 3' TALEN. Target sequences were selected so that there was a 17 bp spacer for *irx7* and a 20 bp spacer for *irx5a*. In vitro transcription of ARCA-capped RNA was performed using the mMESSAGE mMACHINE® T7 Ultra Kit (Life Technologies). Founders for mutant lines were generated by injection of RNA at the one-cell stage. Founders were then outcrossed to wild-type fish to make the F1 generation.

Primers and restriction enzymes for genotyping protocols

Primer Name	Sequence	Amplicon length (bp)	Restriction Enzyme	Length of fragments after digest (if WT)
irx7genot_fwd3	ATGCCTGCTTCATCAACGGG	159	EcoRV	92, 67
irx7genot_rev3	CGGTATTCCTGAGAAAGGTAAGGG			
irx5a_TALENgenot_fwd	TGCTGGCTTTTGAGTGTTTG	311	BsaI	188,123
irx5a_TALENgenot_rev	ATGGCCAGCATGATCTTCTC			

Retroviral transduction

Retroviral transduction was performed using plat-E cells as described previously (Takahashi et al., 2007). Briefly, plat-E cells were plated on gelatin-coated 10cm dishes the day before transfection. On the day of transfection 10.8 ug of plasmid was transiently transfected into plat-E cells using PEI. 24 hours after transfection, the media was removed and replaced with 7.5ml of fresh media. 48 hours after transfection the first batch of virus was collected and filtered and used to transduce ATDC5 cells. 1.25 ml of virus was used per 10 cm dish of ATDC5 cells. Plat-E cells were replaced with fresh media after collecting the first batch of virus. The second batch of virus was collected for transduction at 72 hours. GFP expression was used to monitor transfection efficiency. The efficiency was typically more than 80%. 600,000 ATDC5 cells were then plated on a 10cm dish. 48 hours after plating the cells were transduced with 1.25ml of plat-E virus (per 10cm dish) with polybrene. The plat-E virus was added once more at 72 hours. At 96 hours, media-containing virus was removed and replaced with fresh ATDC5 media.

ATDC5 cell culture and in vitro cartilage differentiation assay

Cells were cultured in growth medium (DMEM/F-12, 5% (v/v) heat-inactivated fetal bovine serum, (100U/ml)/(100μg/ml) penicillin/streptomycin) in a 37˚C humidified incubator at 5% CO_2. Cells were disassociated with 0.25% Trypsin/2.21 mM EDTA and rinsed in media before FACS. The cells were harvested for FACS 48 hours after the second batch of virus was added. For cartilage induction, growth medium was supplemented with 1% ITS + Premix (BD 354352), 100μg/ml ascorbic acid, 100nM dexamethasone, and 10ng/ml TGF-beta 1 (Weiss et al., 2012). For Alcian blue staining,

samples were fixed in 4% PFA for 10 minutes then rinsed 3x in DPBS. Afterward, they were incubated overnight with 0.02% Alcian Blue 8GX (Sigma A5268) in 3% glacial acetic acid in deionized water at room temperature. Then the samples were rinsed three times with deionized water and imaged on a Nikon AZ100 microscope. To quantify alcian blue content of the micromass cultures, the stain was extracted by overnight incubation with 6M Guanidine hydrochloride at room temperature. Absorbance was then measured at 620 nm by spectrophotometry (Newton et al., 2012). For RT-PCR, total RNA was extracted from three micromasses per condition with RNeasy Plus Mini Kit (QIAGEN). cDNA was constructed by RETROscript Kit (Ambion) using 1 µg RNA per reaction. Resulted cDNA was then diluted 6 times and 2 µl of that was used for each qPCR reaction. qPCR was performed using iTaq™ Universal SYBR® Green Supermix (Bio-rad), per manufacturer instructions, on an Applied Biosystems ViiA™ 7 Real-Time PCR System. For each condition (i.e. GFP, IRX1, and Irx7 overexpression) qPCR was done with three technical replicates for each of the three biological replicates. Analysis of the qPCR data was done as described previously (Schmittgen and Livak, 2008). To ensure that PCR conditions yield high efficiency, a standard curve was made for each gene using a serial dilution of the cDNA. All genes had PCR efficiency in the acceptable range for $\Delta\Delta C_T$ method (1.8× to 2.2×). To make sure that the transgene expression was maintained in micromasses after 7 days of culture, RT-qPCR was performed for *Irx1*, *irx7*, GFP and *Gapdh*. Since GFP is expressed as a part of the transgenic construct in all three conditions, GFP expression level was used as a proxy to compare the level of transgenic overexpression between samples. As represented in the

graph below, normalized expression level of GFP (i.e. $2^{-\Delta CT}$) for GFP, IRX1, and Irx7 misexpression samples were 0.0326±0.0049, 0.0176±0.0024 , 0.0362±0.0054 , respectively (Mean±SEM). This shows that similar levels of GFP transcript is present in Irx7 misexpression and GFP control conditions, while IRX1 misexpression was at two-fold lower levels.

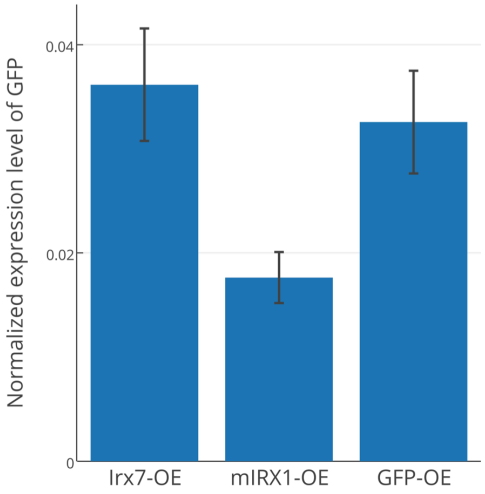

We also compared expression level of Irx1 between GFP control and IRX1 overexpressing samples to show higher levels of Irx1 in the latter. Normalized expression level of Irx1 in GFP and IRX1 misexpression samples were 0.0003± 9.8×10^{-6} and 0.7111± 0.2054, respectively (Mean±SEM). This shows that Irx1 is expressed at much higher levels in its corresponding sample compared to the control. Normalized expression level of irx7 in Irx7 overexpression samples was 1.928±0.0816 (Mean±SEM), whereas in the other samples no specific irx7 PCR product was detected. These results are summarized in the graph below.

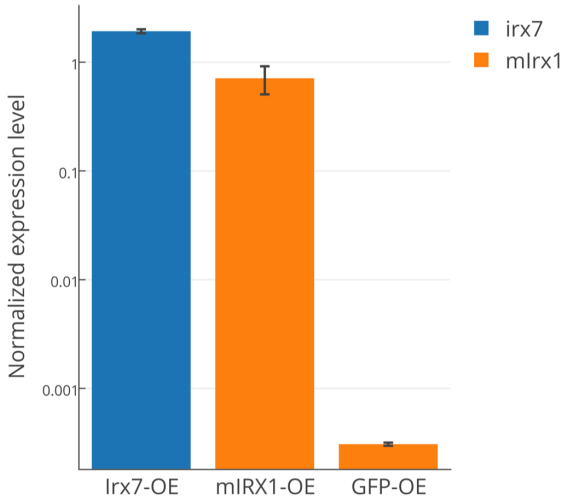

Fold changes were calculated as $-1/2^{-\Delta\Delta CT}$. To test whether changes in the expression level are statistically significant, a one way ANOVA followed by Tukey HSD test was performed on the normalized expression level of each gene, comparing the expression level in the GFP control samples with Irx7 and IRX1 overexpression samples. See Table S2 for information on primers used for qPCR.

Primers for qPCR

Gene	Primers	Amplicon size
Acan	fwd: GCATGAGAGAGGCGAATGGA rev: CTGATCTCGTAGCGATCTTTCTTCT	144 bp
Col2a1	fwd: AGAACATCACCTACCACTGTAAGAACA rev: TGACGGTCTTGCCCCACTT	189 bp
Trps1	fwd: GAGATCTCGAGACACTACAG rev: CTCTTCGCCATTAGCAGTAG	147 bp
Sox9	fwd: TCTGGAGGCTGCTGAACGA rev: TCCGTTCTTCACCGACTTCCT	131 bp
Gapdh	fwd: TGCACCACCAACTGCTTAG rev: GATGCAGGGATGATGTTC	176 bp
Irx1	fwd: CAGCGCCTTCTTGCCCTAT rev: CCGGGGTTGTCCTTCAGTT	81 bp
irx7	fwd: ACCGGGCTACAGTTTCATCC rev: TAGTATGGTCCTCCCCGTCC	123 bp
GFP	fwd: AAGTTCATCTGCACCACCG rev: TCCTTGAAGAAGATGGTGCG	173 bp

In situ probe templates

Probe	Primer sequence/Template	Restriction enzyme to linearize the plasmid	RNA polymerase for riboprobe synthesis
irx7	Fwd: CCGTATCACCAAGCTCTCCT Rev: TGACGGACTCAAAGTGCAAG	PstI	SP6
irx5a	Fwd: TAAAAGAAGCAGAGGAGCGGACG Rev: AATACAAATAGACTCAGGCGGCTG	BamHI	T7
col2a1a	Fwd: GTAAAGATGGAGAGACTGGACCTTC Rev: ATTCTCTCCTCTGTCTCCCTGTTT	NotI	SP6
acana	Fwd: TGTGAACCAAACCCTTGTGGAGC Rev: CGAAGGCTTGCTCCTCTGGAG	NotI	SP6
irx1b	Fwd: GGAGAATAAAGTGACCTGGGG Rev: CCGATGACGTATATGCTGTTGC	NotI	SP6
mIrx1	Dharmacon, EST Partially Sequenced Mouse Irx1 cDNA (CloneId:6404582)	EcoRI	T3

Sequences of modified R2 enhancers and probes for EMSA

Enhancer sequences	
R2	CCTCTGACACCTGATGCCAATTGCGGTCAGTGTTTTGCTGGC GACACAGATTCTTGTGCCAATGGCCAGGCCCCTCATCATCTG ATCCGCAGCAACCCAGCCACCCTACACACCCCTGGAGCCTCT CCGTGTTCTCCTCATCCCTCTACCTTTCCGCACTCTCCCTCCA TCCACACCCGCGGCTCTCTTCTCCCCCACTGCCCGGTGCTCT CTCACATTCCTCAGGTCTGCACACAGAGCCGCATTGTGTGTG TGTCTTACAGAGCACACAGTCAGGGCTCATTTCGGACACACA CACACATCCAACAGGGTGTGTGCACAGTCGCAGCGATGCGT ACACACACATACACATATCCCT
R2-ΔIrx$_{2-4}$	CCTCTGACACCTGATGCCAATTGCGGTCAGTGTTTTGCTGGC GACACAGATTCTTGTGCCAATGGCCAGGCCCCTCATCATCTG ATCCGCAGCAACCCAGCCACCCTACACACCCCTGGAGCCTCT CCGTGTTCTCCTCATCCCTCTACCTTTCCGCACTCTCCCTCCA TCCACACCCGCGGCTCTCTTCTCCCCCACTGCCCGGTGCTCT CTCACATTCCTCAGGTCTGCACACAGAGCCGCATTGTGTGTG TGTCTTACAGAGCACACAGTCAGGGCTCATTTCGG---------- TCCA---------GTGCACAGTCGCAGCGATGCGT--------- TACACATATCCCT
R2-Δsox/Irx$_1$	CCTCTGACACCTGATGCCAATTGCGGTCAGTGTTTTGCTGGC GACACAGATTCTTGTGCCAATGGCCAGGCCCCTCATCATCTG ATCCGCAGCAACCCAGCCACCCTACACACCCCTGGAGCCTCT CCGTGTTCTCCTCATCCCTCTACCTTTCCGCACTCTCCCTCCA TCCACACCCGCGGCTCTCTTCTCCCCCACTGCCCGGTGCTCT CTCACATTCCTCAGGTCTGCACACAGAGCCGCAT----------

	CTTACAGAGCACACAGTCAGGGCTCATTTCGGACACACACAC ACATCCAACAGGGTGTGTGCACAGTCGCAGCGATGCGTACA CACACATACACATATCCCT
R2-Δsox/Irx$_1$ + Sox9	CCTCTGACACCTGATGCCAATTGCGGTCAGTGTTTTGCTGGC GACACAGATTCTTGTGCCAATGGCCAGGCCCCTCATCATCTG ATCCGCAGCAACCCAGCCACCCTACACACCCCTGGAGCCTCT CCGTGTTCTCCTCATCCCTCTACCTTTCCGCACTCTCCCTCCA TCCACACCCGCGGCTCTCTTCTCCCCCACTGCCCGGTGCTCT CTCACATTCCTCAGGTCTGCACACAGAGCCGAACAAAGGGG CCTTTGTCTTACAGAGCACACAGTCAGGGCTCATTTCGGACA CACACACACATCCAACAGGGTGTGTGCACAGTCGCAGCGAT GCGTACACACACATACACATATCCCT
R2-Δirx$_1$	CCTCTGACACCTGATGCCAATTGCGGTCAGTGTTTTGCTGGC GACACAGATTCTTGTGCCAATGGCCAGGCCCCTCATCATCTG ATCCGCAGCAACCCAGCCACCCTACACACCCCTGGAGCCTCT CCGTGTTCTCCTCATCCCTCTACCTTTCCGCACTCTCCCTCCA TCCACACCCGCGGCTCTCTTCTCCCCCACTGCCCGGTGCTCT CTCACATTCCTCAGGTCTGCACACAGAGCCGCATTGT-------- CTTACAGAGCACACAGTCAGGGCTCATTTCGGACACACACAC ACATCCAACAGGGTGTGTGCACAGTCGCAGCGATGCGTACA CACACATACACATATC

Sequence of probes used for EMSA

Probe name (sign in Figure 4B)	Sequence
R2_1 (+)	GTCTGCACACAGAGCCGCATTGTGTGTGTGTCTTAC AG
R2_1_ΔSox/Irx (Δ)	GTCTGCACACAGAGCCGCATCTTACAG
R2_1_ ΔIrx (Δ')	GTCTGCACACAGAGCCGCATTGTCTTACAG
R2_1_ ΔSox/Irx+sox9 (S)	GTCTGCACACAGAGCCGAACAAAGGGGCCTTTGTCT TACAG

In situ hybridization on sections

Limbs of mouse embryos at E14.5 were dissected in cold PBS and fixed in 4% PFA overnight at 4°C. Tissues were then embedded in OCT and frozen on dry ice. In situ hybridization was performed on sections as previously described (Schipani et al., 1997). See Table S2 for sequences of anti-sense riboprobes.

Supplementary References

Newton, P.T., Staines, K.A., Spevak, L., Boskey, A.L., Teixeira, C.C., Macrae, V.E., Canfield, A.E., and Farquharson, C. (2012). Chondrogenic ATDC5 cells: an optimised model for rapid and physiological matrix mineralisation. International journal of molecular medicine *30*, 1187-1193.

Schipani, E., Lanske, B., Hunzelman, J., Luz, A., Kovacs, C.S., Lee, K., Pirro, A., Kronenberg, H.M., and Juppner, H. (1997). Targeted expression of constitutively active receptors for parathyroid hormone and parathyroid hormone-related peptide delays endochondral bone formation and rescues mice that lack parathyroid hormone-related peptide. Proceedings of the National Academy of Sciences of the United States of America *94*, 13689-13694.

Singh, S.P., Holdway, J.E., and Poss, K.D. (2012). Regeneration of amputated zebrafish fin rays from de novo osteoblasts. Dev Cell *22*, 879-886.

Weiss, H.E., Roberts, S.J., Schrooten, J., and Luyten, F.P. (2012). A semi-autonomous model of endochondral ossification for developmental tissue engineering. Tissue engineering Part A *18*, 1334-1343.